ISSN 1070-3632, Russian Journal of General Chemistry, 2013, Vol. 83, No. 13, pp. 2676–2685. © Pleiades Publishing, Ltd., 2013.
Original Russian Text © N.N. Rozhkova, 2012, published in Ekologicheskaya Khimiya, 2012, Vol. 21, No. 4, pp. 240–251.

Aggregation and Stabilization of Shungite Carbon Nanoparticles

N. N. Rozhkova

Institute of Geology, Karelian Research Center, Russian Academy of Sciences,
Pushkinskaya ul. 11, Petrozavodsk, 185910 Russia
e-mail: rozhkova@krc.karelia.ru

Received December 26, 2012

Abstract—Globular clusters of natural shungite carbon appear to be aggregates formed by nonplanar graphenes through stable aqueous dispersion. The ability of the clusters for spontaneous disaggregation in water and stabilization without surfactants was demonstrated. Due to their size and curvature, shungite graphenes contribute most substantially to stabilization of the carbon clusters in water and predetermine amphiphilicity of shungites. The condensation of aqueous shungite nanocarbon dispersion is accompanied by formation of a three-dimensional network with characteristic micro- and submesopores of <0.7–5.0 nm. The pore structure is distinguished by a changeable sorption capacity due to mobility of the graphene fragments forming the pore walls.

Keywords: Shungite carbon, nonplanar graphene, aqueous shungite nanocarbon dispersion, aggregation, stabilization of carbon nanoparticles, physicochemical properties.

DOI: 10.1134/S1070363213130136

INTRODUCTION

Carbon-rich shungite rocks (shungites) attract interest as a promising carbonaceous material and as a source of nanodispersed carbon [1]. Natural nanocarbon reflects the global carbon cycle processes and is part of soils and sediments, which fact complicates the analysis of its structural and physicochemical properties. Also, metastable and nongraphitizable shungite carbon (ShC) is contained in virtually all rocks of Karelia, differing in genesis and composition, and is found over an area of over 9000 km^2 in amounts of up to 25×10^{10} tons. To date, there is no consensus on the origin of ShC [2], but, according to geological data, shungite rocks were formed in water, which finding creates further problems in studies of nanocarbon, associated with interaction of the carbon nanoparticles (NPs) with water and their aggregation.

Aggregation of NPs represents a topical scientific issue pertinent to all new-generation carbon materials, including fullerenes, nanotubes, nanodiamonds (NDs), and graphenes due to their high-surface area and reactivity. All the physicochemical processes, mass and heat transfer on the nanoparticles proceed at enhanced rate, and strengthening of the inter-nanoparticle interaction and aggregation of NPs complicate controlling these processes. Efficient use of NPs requires knowledge of their stabilization conditions, since aggregation occurs already in their formation stage, thereby leading to the loss of activity [3].

The main driving force behind aggregation and coagulation of nanoscale particles is a decrease in the excess surface energy. The theory of stability of colloidal systems (DLVO) takes into account the electrostatic repulsion energy and the molecular energy of attraction of the particles in solution; in some cases the structural and mechanical (steric) factor of adsorbed layers is included as a stabilizer, and the entropy factor of excluded volume (depletion) effects, as a destabilizer of the colloidal state. Formation of aggregates is limited by their diffusion rate in the dispersion medium [4].

Aggregation and/or crystallization of NPs and the morphology of the resultant phase are determined by the mechanisms of molecular convergence, reorientation, and association, which are controlled by both long-range colloidal interaction forces and short-range pair interaction potential [5].

It was suggested [6] that the structure and dynamics of formation of the nanoscale carbon network be described on the basis of a comparative study of

morphologically and genetically similar fullerene-like particles and C_{60}. This approach was applied to the nanostructures constituting the matrix of ShC and determining its properties [7].

With opening up the possibilities for directed modification of properties at different structural levels, from mesoscopic to atomic, a new subject for theoretical and experimental research was found in graphenes, two-dimensional hexagonal sheets forming graphite [8, 9]. However, practical application of graphenes is limited by the fact that mass production of high-quality graphene samples remains an unsolved problem. Thermal expansion of graphite is being discussed as one of the most easily available methods of their preparation [10]. Also proposed was a method of chemical reduction of graphene oxide which, in turn, can be obtained by prolonged ultrasonic treatment of oxidized graphite in water.

Carbon NPs are synthesized via high-temperature, energy-intensive processes (detonation nanodiamonds), in a controlled inert atmosphere (fullerenes and nanotubes). The resulting carbon products need additional chemical treatment: extraction of fullerenes with organic solvents from fullerene soot; acid treatment of diamond blend to remove impurities and amorphous carbon, etc. Purification of carbon NPs employs mostly "wet chemistry" methods, which necessitates addressing the problem of interaction of carbon NPs with water and solutions.

Similar problems arise in processing of high-carbon shungite rocks using traditional technologies, which do not control the contribution from nanostructured components, with the result being a strong variation of the properties of shungite-containing materials depending on the method of preparation and storage conditions. Two procedures were proposed for stabilizing the composition and properties of high-carbon shungites. One procedure is based on a high-temperature treatment leading to fundamentally new materials comprised of a mixture of silicon carbide and hyperfullerene carbon [11]. The other procedure employs the traditional approach (which previously received practical approval in the case of liddites), based on the use of powerful chemicals and autoclaving treatment for removing mineral components of shungites and carbon concentrating [12, 13]. However, both procedures yield nanostructured products represented by heterogeneous strong aggregates. Moreover, the modified products lack amphiphilicity [i.e., the ability to be attracted by both nonpolar (organic) and polar (above all water) environments], which is the main property differentiating shungite out from other natural and synthetic carbon materials.

Here, we analyzed the results of a comprehensive study of the structure of ShC, which allows addressing the issues of aggregation and stabilization of carbon nanoparticles. These results are of particular importance in view of the projected widespread use of high-carbon shungite rocks for water treatment purposes, as well as for environmental and biomedical applications, whereas the interaction of carbon NPs with water is a new issue, inadequately addressed in scientific literature.

Aqueous Dispersions of Carbon Nanoparticles

Stable aqueous dispersions of hydrophobic carbon NPs synthesized in an inert atmosphere (fullerenes, nanotubes, fullerene soot, nanodiamonds, and nanographites) can be prepared only after their modification. An important role in stabilizing, e.g., colloidal graphite particles in water belongs to oxygen-containing groups on the carbon particle surface [14]. These groups result from oxidation of graphite ground to colloidal sizes in a vibrating mill using a mixture of HNO_3 and H_2SO_4 acids. Rinsing the oxidized powder with water causes the exchange of salt-like functional groups for hydroxy groups via hydrolysis. Such oxidation provides for sufficient solvation and colloidal dissolution of the graphite particles in liquids with the dielectric constant ≥ 15 (water, acetone, alcohols, with acids excluded). Reduction of the average size of the graphite particles in an aqueous solution is achieved through prolonging the milling time due to oxidation of carbon and adsorption of intracrystalline water. Hydration of the carbon NPs is regarded as the main stabilizing factor for hydrophobic particles in water. It should be noted that widespread use of aqueous dispersions of colloidal graphite is limited by low pH values, 2.4–2.8 [15].

Like in the case of graphite, acid treatment of natural and synthetic diamonds in aqueous dispersions leads to imparting a negative charge to the microparticles due to dissociation of the functional, predominantly acidic, groups [16].

In the alkaline pH range at low electrolyte concentrations ($<10^{-3}$ M KCl) the aggregation stability of aqueous dispersions of natural and synthetic diamonds is due to the electrostatic factor and is well

described by the DLVO theory. The height of the electrostatic barrier exceeds 100 kT, and the depth of the far-lying minimum is negligible.

For acid media, at potassium chloride concentrations above 10^{-2} M, the DLVO theory treats the molecular attractive forces as dominating at all interparticle distances [17]. The lack of aggregation of natural diamond particles, observed at pH 2 and KCl concentrations to 0.5 M, is due to the structural component of the disjoining pressure, which limits the depth of the near-lying potential well.

In recent years, certain interest has been shown in studying aqueous dispersions of graphene oxide, obtained from differently modified graphene [18].

A distinctive feature of aqueous dispersions of fullerenes is a close to neutral pH value. Several mechanisms were invoked to explain the stabilization of fullerene clusters in water: the occurrence of oxygen-containing groups on surface defects, formation of charge-transfer complexes, and hydration effects [19]. Among these mechanisms, hydration via formation of donor-acceptor complexes of water molecules with fullerene underlies the most widely accepted model [20, 21].

The situation becomes more complicated when amphiphilic particles, including shungite carbon NPs containing, along with nonpolar portions, polar and charged functional groups, are dissolved in water [22]. Below we present some data on modification of ShC in water aimed at shungite NP stabilization.

Shungite type I powders from Shun'ga deposit (particle size <40 μm, 96 wt % carbon) were used for preparation of aqueous dispersions by ultrasonic treatment according to the procedure described in [23], followed by filtration and centrifugation. The shungite powder left on the filter after filtration of an aqueous colloid is represented by fairly large particles ranging in size from fractions to tens of micrometers. We had to find the optimum procedure for treating the powder to remove mineral impurities and increase the degree of dispersity of NPs in water.

To remove traces of silica (the main impurity) the shungite powder was treated with a mixture of hydrochloric and hydrofluoric acids. However, the powder was not released into water by subsequent ultrasonic dispersing. Ozonation for 2, 4, and 15 h by the procedure described in [24] allowed transforming the powder to an aqueous dispersion. The size of the particles in the dispersion before and after ozonation was determined by the dynamic light scattering (DLS) on a Zetasizer Nano ZS nanoparticle size analyzer (Malvern Instruments) and transmission electron microscopic (TEM) techniques.

The dispersions obtained by the ultrasonic treatment of the initial shungite powder were characterized by the concentration of ~0.1 mg/mL and, according to the DLS data, by the average size of the carbon particles of ~98 nm (against 35 nm for the clusters in aqueous dispersions of fullerenes, obtained by the same procedure). Individual particles in the precipitate ranged in size from 10 to 400 nm, according to the TEM data [25]. After the acid treatment and subsequent ozonation of the shungite powder, the average size of the nanoclusters increased to 326 nm. The polydispersity of the clusters also increased. Prolonged ozonation of the shungite powder allows not only transforming ShC to an aqueous dispersion but also obtaining a stable dispersion of the nanoparticles at a higher NP concentration in the dispersion [26].

Treatment by the above-described procedures allows removal of mineral impurities, and the resulting morphostructure of the precipitates is dominated by smaller particles with a size of 20–100 nm. However, ozonation causes an undesirable decrease in pH to 2 in the dispersion.

Of greatest interest are the conditions under which carbon NPs can be stabilized without oxidation and which provide for sufficient solvation and dissolution of colloidal particles, without impurity salts or surfactants, as exemplified by aqueous dispersions of hydrated fullerenes.

We carried out a comparative study of aqueous dispersions of carbon NPs, prepared from shungite, fullerene, and nanodiamond powders without using surfactants. As objects of study served type I shungite powder (Shun'ga deposit), a fullerene powder containing C_{60}/C_{70} = 83/16 and ~1 wt % higher fullerenes (Intellect Co., St. Petersburg), and nanodiamond samples which were kindly provided by Prof. E. Ōsawa (NanoCarbon Research Institute Ltd., Japan).

Dispersions were prepared by treatment on a UZ-2M ultrasonic disperser by the procedure described in [23]. The resulting mixtures were filtered through a blue ribbon filter and centrifuged on a RotinaR centrifuge for 30 min at 7000 rpm speed.

Silica, which is the main impurity passing from type I shungite to water, was removed from the aqueous dispersion of ShC by treatment of the powder left on the filter, repeated in quintuplicate. The resulting aqueous dispersions of ShC are comparable in the content of impurities with the synthetic nanocarbon materials examined, as seen from the mass-spectrometric data (ICP MS analysis) presented in Table 1.

We obtained stable aqueous dispersions for fullerenes, ShC, and NDs but failed to obtain an aqueous dispersion from a graphite powder under identical conditions.

Aqueous dispersions of ShC with the concentration of 0.1 mg/mL were opalescent, with a gray-brown color. The average size of the clusters in water as determined by the DLS technique was ~50 nm at pH of the dispersion of 6.3–6.8. The size distribution of the ShC nanoparticles is presented in Fig. 1. The TEM examination revealed the presence of particles with sizes from 5 nm and their aggregates to 100 nm (Fig. 2).

Despite aggregation of the structural elements in an aqueous medium, the average size of the carbon clusters increases more than 5 times for all the carbon nanoparticles (Table 2); the sedimentation stability of the dispersions is preserved for several years.

Table 1. Elemental composition of the aqueous dispersions of the nanocarbon materials[a]

Elements	Water (control), μg/mL	Fullerene, μg/mL	ND, μg/mL	Sh-I, 5 times, μg/mL
Mn	Not detected	Not detected	0.0031	< 0.031
Na	0.215	1.54	1.24	1.92
K	0.09	0.017	1.83	0.29
Co	0.022	0.018	0.021	0.03
Ni	0.0055	0.007	0.0016	0.03
Cu	Not detected	0.034	0.0024	0.054
Zn	0.024	0.027	0.018	0.022
Li	Not detected	Not detected	0.0066	< 0.012
Rb			0.018	0.018
Cs			0.010	0.00451

[a] The Zr contamination introduced by grinding bodies in the disaggregation technology is not included.

Role of Hydration in Stabilization of Aqueous Dispersions of Carbon Nanoparticles

In the context of preparation of aqueous dispersions of carbon nanoparticles, the mechanisms of their aggregation stability constitute an issue of great relevance. It should also be taken into account that aggregation involves formation of a polycrystalline or amorphous fullerite able to more actively interact with water than does the initial carbon material; similar morphological structures (globular) result from condensation of ShC, fullerene, and ND dispersions.

It was presumed that the main role in the specific interaction of ShC with water belongs to the basic structural units (BSUs) <1 nm in size, represented by stacked curved graphene layers forming cups, which presumption is consistent with the data obtained for fullerenes and nanotubes. It was shown previously [27] that the deformed, nonplanar structures differentiating fullerenes and nanotubes from graphites predetermine high reactivity of the fullerene structures [27]. Two types of adsorbed water were detected in single-walled nanotubes: water inside nanotubes and water adsorbed

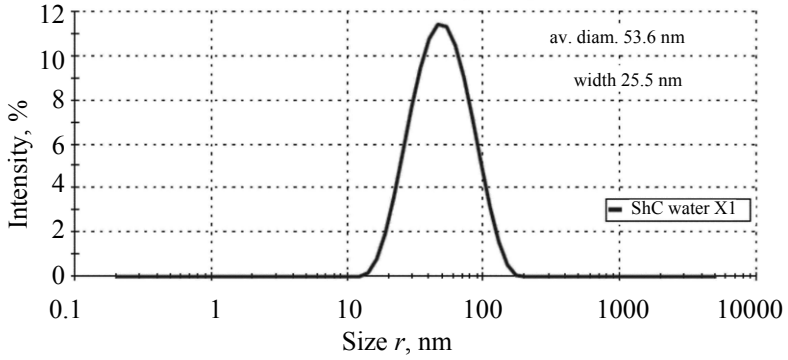

Fig. 1. Pore size distribution of the carbon shungite clusters in the stable aqueous dispersion according to DLS data.

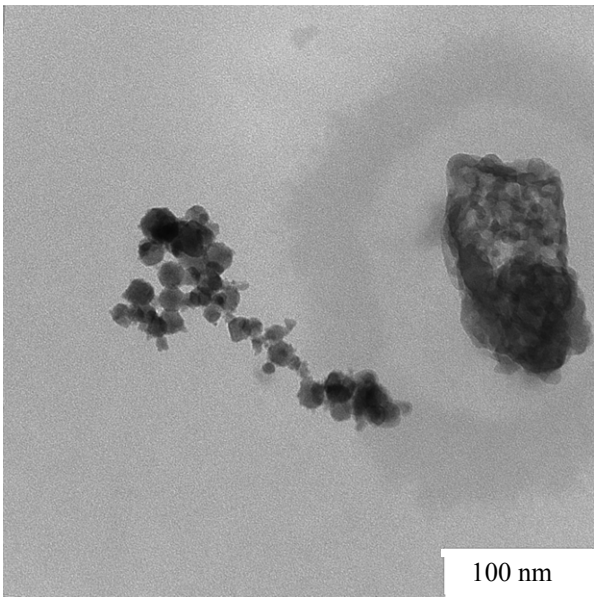

Fig. 2. TEM micrograph of the shungite carbon nanoparticles prepared by drying the stable aqueous dispersion.

at nanotube defect sites. The water binding energy depends on the graphene surface curvature, with the hybridization changing from sp^2 to an intermediate state between sp^2 and sp^3 [28, 29].

The formation of specific hydration structures preventing fast coagulation of nanoparticles is one of the major factors of at least kinetic, if not thermo-dynamic, stability of the dispersions. We examined the state of the water bound to fullerenes and ShC nano-clusters by the ESR spin probing (with hydrophilic 4-Oxo-TEMPO), as well as by high-resolution solid-state NMR and pulsed-field gradient NMR techniques [30–32].

In the ESR experiments we observed the pattern of variation of the properties of "nonfreezing" water, whose proportion decreases with decreasing temperature. The sequence of freezing for water fractions is as follows: water localized near nonpolar (at temperatures from –10 to –20°C) and then water localized near polar and charged groups (at temperatures from –70 to –90°C). For the "bulk" water the same signal was observed in the systems examined at identical temperatures. Strong reduction in mobility of the probe due to bulk water freezing ($T < 260$ K) causes broadening of the spectra and manifestation of signals from probes localized in the layer of nonfreezing water with the highest mobility near the surface of nanoclusters [30].

A fairly broad solid-state ^{1}H NMR spectrum (Fig. 3) recorded for the ShC sample obtained by drying from an aqueous dispersion consists of two peaks, at 0.40 and 3.16 ppm, which were attributed to the water molecules interacting with ShC.

The signals from the OH groups grafted to fullerenes were detected in fullerols at 1.2, 1.5, and 1.8 ppm. The OH groups involved in hydrogen bonding in a water molecule are characterized by a stable signal at 7 ppm. The spectrum of fullerols displays a downfield shift of the signal from the OH group at 0.9 ppm, which characterizes their hydrophilic properties. By analogy, for ShC the peak at 0.40 ppm was associated with water complexes on the basic structural units (nonplanar) constituting the ShC clusters, and the peak at 3.16 ppm, with the adsorbed bulk water [31].

Using the pulsed-field gradient NMR data, the self-diffusion coefficients (D) and the weight fractions (p) were determined for these samples: $D_{s1} = 4\times10^{-9}$ m^2/s, $p_1 = 0.06$ and $D_{s2} = 2.1\times10^{-9}$ m^2/s, $p_2 = 0.94$. The former component corresponds to the water bound to the ShC nanoparticles, and the latter component, to bulk water. The exchange rate between these states of water is 5 ms [32]. These results are generally consistent with the ^{1}H NMR spectral features observed for ShC.

Table 2. Average size of the carbon nanoparticles in the stable aqueous dispersions according to the DLS data

Samples	Average size of the structural unit, nm	Concentration of the nanoparticles, mg mL^{-1}	Average radius of the nanoparticles in the aqueous dispersion, nm	Polydispersity
ShC	Globular cluster <6	0.024	50.0	0.41
ShC	Multilayer aggregate <6	0.048	52.0	0.28
C_{60}/C_{70}	Average diameter of the C_{60} molecule 0.7	0.027	36.8	0.42
ND	ND core diameter 4.5	0.24	26.4	0.30

Effect of Water on the Properties of Nanocarbon

Studies of the electronic structure and electrophysical properties of nanographite showed that they can be reversibly altered by water vapor sorption [33]. Deformed structures differentiating fullerenes from graphites predetermine high reactivity of the fullerene structures. Jumps and flat gradients observed in the temperature dependences of the specific heat, thermal conductivity, thermoelectric power, and electrical conductivity of shungite nanocarbon are associated with water desorption from the nanosized pores formed by nonplanar BSUs of shungite carbon [34].

The ^{13}C NMR, small-angle neutron scattering, and small-angle X-ray scattering examinations confirm a two-level structural organization of both pores and structural units of shungite carbon in the 1–100 nm range. Using high-resolution transmission electron microscopy it was possible to visualize <6 nm globular clusters formed by nonplanar graphenes (NGs) with sizes below 1 nm. The size and surface curvature of the BSUs of ShC determine its electronic structure and dipole moment, as reflected in amphiphilicity of ShC, and also play an important role in stabilization of carbon NPs in water [23, 35].

The dipole moment of the structural units of shungite carbon was calculated using the measured static dielectric polarization data for the NGs in dilute benzene, toluene, and o-xylene solutions at temperatures within 25–60°C [36]. The dipole moment of the NGs in benzene, estimated at 6.5 D, indicates that, even in very dilute solutions, NGs occur in the form of clusters which are stabilized due to mobility of nonplanar fragments.

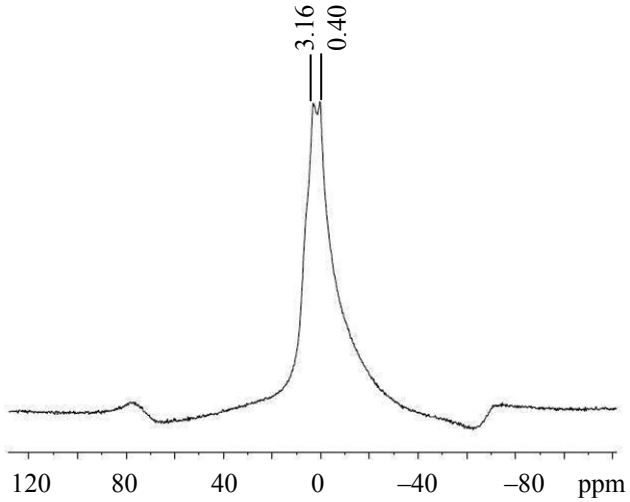

Fig. 3. Solid-state ^{1}H NMR spectrum of the shungite carbon sample obtained through condensation of the aqueous dispersion (sample rotation frequency 35 kHz).

Structural Organization of Shungite Carbon

Atomic-force and scanning microscopic examinations revealed formation of a two-dimensional network of nanoparticles through dispersion precipitating and drying. The pore structure of ShC was characterized by adsorption methods. The pore size distribution was estimated from the low-temperature nitrogen adsorp-

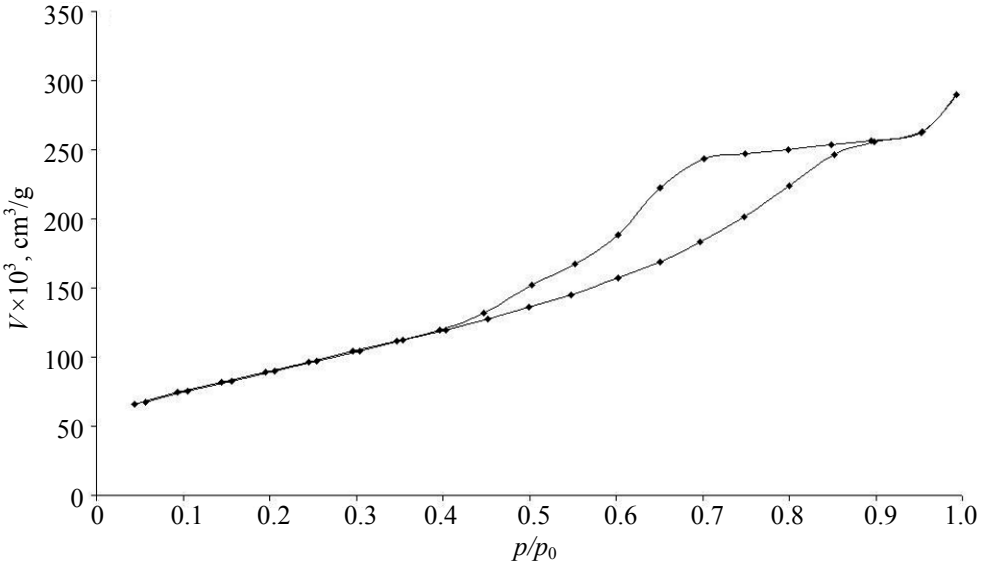

Fig. 4. Low-temperature nitrogen adsorption isotherm for the powder obtained through condensation of the stable aqueous dispersion of shungite carbon.

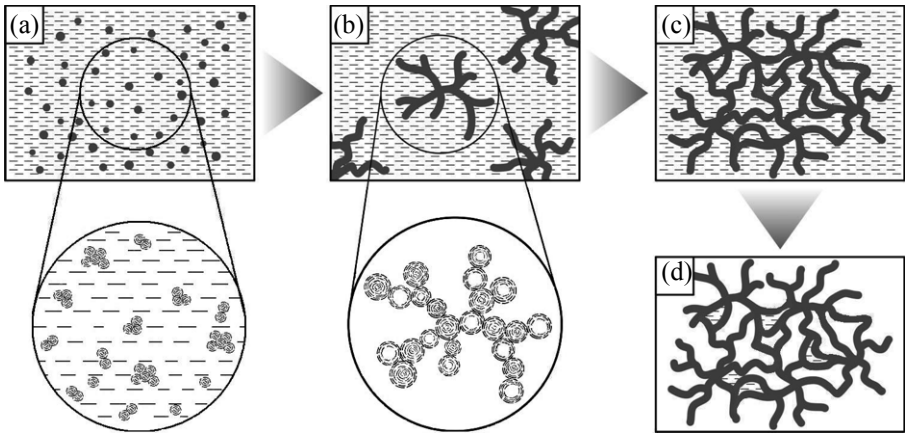

Fig. 5. Scheme of clusterization of the graphene fragments of shungite carbon in aqueous dispersion condensation: (a) dilute dispersion 0.1 mg mL^{-1}, (b) dendritic clusters upon increasing the dispersion concentration, (c) network formed through condensation of the dispersion, and (d) after drying the dispersion, water remains in the clusters and characterizes the intergraphene interaction.

tion isotherms (BET method), determined using a Quantachrome instrument with an Autosorb 1C automatic analyzer. The micropore volume and radius were calculated by the Dubinin-Radushkevich equation. The volume of ultramicropores (pore width 0.33–0.7 nm) was estimated from CO_2 adsorption data, and the total micropore volume (pore width <2 nm), from nitrogen adsorption isotherms [37, 38].

The adsorption isotherm of the carbon obtained from a stable aqueous dispersion of ShC exhibits a type IV curve with a hysteresis in the desorption isotherm, characteristic of a mesoporous sample (carbon network) (Fig. 4). Similar isotherms were described for montmorillonite nanoclay distinguished by a changeable sorption capacity due to mobility of the nanoparticles forming the pore walls. In shungite carbon, nonplanar graphenes are responsible for changes in the sorption capacity.

A narrow hysteresis (to $p/p_0 = 0.4$) is indicative of the presence of 2–5-nm mesopores. The average pore radius (BET) was estimated at 2.5 nm, the maximum pore size being <21.2 nm (at $p/p_0 = 0.95$). As seen from Table 3, the ShC with nanoparticles obtained through stabilization of an aqueous dispersion is characterized by larger specific surface area and specific volume of meso- and micropores.

The pore size distribution data, obtained by adsorption techniques for the three-dimensional carbon network resulted from condensation of the aqueous dispersion, lend evidence in support of the structure of

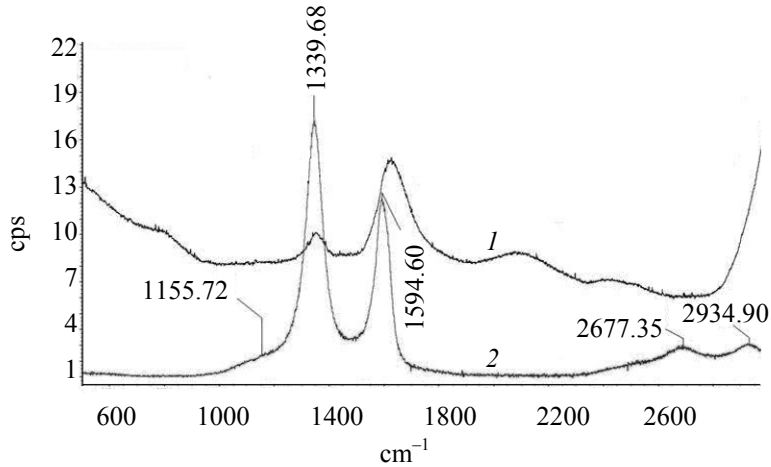

Fig. 6. Raman spectra of the shungite carbon clusters in the aqueous dispersion (*1*) before and (*2*) after condensation; 532 nm laser excitation.

Table 3. Specific surface area (S) and adsorption capacity (V) of the initial ShC and ShC resulted from condensation of the stable aqueous dispersion

Samples	Based on nitrogen adsorption <2 nm		Based on CO_2 adsorption 0.33–0.7 nm		Based on H_2O vapor adsorption	
	S, m^2/g	V, cm^3/g at $p/p_0 = 0.95$	S, m^2/g	V, cm^3/g	S, m^2/g	V, cm^3/g
ShC (Shun'ga deposit)	25.9	0.03	87.7	0.033	200.3	0.10
ShC from the stable aqueous dispersion	325.4	0.45	144.2	0.055	577.7	0.337

the nanoclusters, dominated by micro- and submesopores of <0.7–5.0 nm.

Figures 5b and 5c illustrate the structural transformations caused by condensation of the aqueous dispersion of ShC as accompanied by aggregation of the primary nanoclusters and formation of a three-dimensional network. An important role in these transformations belongs to the BSUs, nonplanar fragments, and their specific interaction with water. Such particles (Figs. 5c and 5d) are able of spontaneous disaggregation in water.

Nonplanar Graphene Fragment

Figure 6 shows the Raman spectra of the stable aqueous dispersion of ShC before and after condensation, recorded on a Nicolet Almega XR (Thermo Scientific) spectrometer. It is seen that the spectra are sensitive to the concentration of the nanoparticles in the dispersion. In the region of the stretching C–C vibrations of the benzenoid rings there are fairly broad doublet bands D and G having comparable intensities, with peaks at 1339 and 1594–1633 cm^{-1}, respectively. The facts that the D band forbidden in regular graphene appears in the Raman spectrum and that the 2D band, allowed in regular graphene, is not observed in the region of the overtone of the G band provide evidence for size-restricted graphene fragments being the scattering object [39].

The interaction of the nonplanar graphenes inside the ShC clusters was described with the use of the Auger spectroscopic data as compared with those for fullerenes, graphite, and onion-like carbon (Fig. 7).

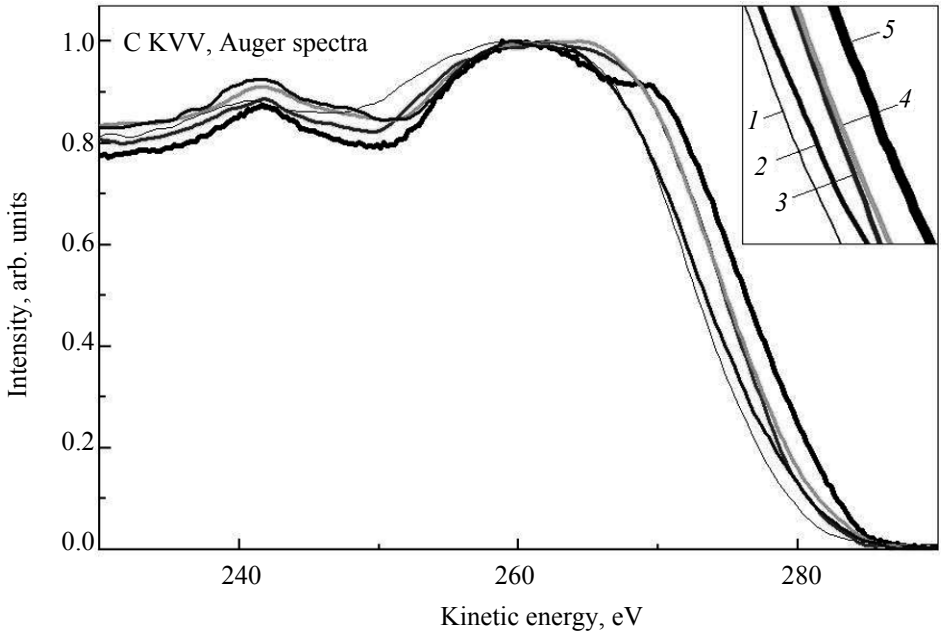

Fig. 7. Intercomparison of the Auger spectra of (*1*) C_{60} fullerene, (*2*) initial shungite carbon, (*3*) condensed aqueous dispersion of ShC, (*4*) onion-like carbon (OLC), and (*5*) graphite. The spectra were recorded by Dr. A.P. Dement'ev. (*1*) C_{60}, (*2*) SH1 (ShC), (*3*) SCH1 ShC from dispersion, (*4*) OLC, and (*5*) graphite.

The right-hand side of the Auger spectrum is associated with π-band electron emission, and the spectra show the difference in the π-bands of the above-mentioned carbon states (inset in Fig. 7). The Auger spectrum of the initial ShC sample coincides with that of fullerene, and the spectrum of the ShC clusters resulted from condensation of an aqueous dispersion, with that of onion-like structures. These findings are indicative of the inter-graphene interaction and confirm the effect produced by the water-graphene interaction on the electronic structure of ShC [40].

The experimental evidence in favor of a graphene-like structural unit was confirmed by quantum-chemical calculations. It was shown that transformation of planar to curved graphene petal can be achieved by one-side adsorption of not only atomic hydrogen but of hydroxyl as well [41, 42]. The initially zeroth dipole moment of the carbon skeleton of the membrane with linear dimensions of 0.8 nm increases to 1.4 and 6.5 D in cases of termination with hydrogen and oxygen, respectively. The latter value is nearly identical to the experimental data, which fact supports the effect produced by oxygen on the formation of nonplanar graphene fragments in ShC and refers stabilization of graphenes in clusters to strong dipole-dipole interaction of the water molecules with the curved graphene membrane.

CONCLUSIONS

Aqueous dispersions of shungite carbon nanoparticles were stabilized in the absence of surfactants and have a close to neutral pH. The average size of the carbon clusters in the dispersion was estimated at 50 nm (dynamic light scattering data) and 5–100 nm (transmission electron microscopic data). The clusters are formed by smaller than 1-nm nonplanar graphene fragments.

Owing to high asymmetry of electron density, nonplanar graphenes exhibit high reactivity, tendency to clustering, large dipole moments (6.5 D), and interaction with water.

Condensation of a stable dispersion leads to formation of a three-dimensional network with micro- and submesopores <0.7–5.0 nm, whose size correlates well with that of nonplanar graphenes and of the main globular clusters of shungite carbon, <6 nm. The pore structure of ShC, resulted from condensation of the aqueous dispersion, is distinguished by a changeable sorption capacity due to mobility of the graphene fragments forming the pore walls.

The graphene-like nature of the basic structural unit of shungite carbon and the effect produced by water on its electronic structure were confirmed by Raman spectroscopy for the ShC nanoparticles in dispersion before and after condensation. These findings are in a good agreement with the results of quantum-chemical calculations for oxygen-terminated nonplanar graphene structures.

Due to their size and curvature, the basic structural units of ShC contribute most substantially to stabilization of carbon nanoparticles in water and predetermine the specific amphiphilicity of shungites.

REFERENCES

1. Rozhkova, N.N., Emel'yanova, G.I., Gorlenko, L.E., and Lunin, V.V., *Ross. Khim. Zh*., 2004, vol. 48, no. 5, pp. 107–115.
2. Buseck, P.R., Galdobina, L.P., Kovalevski, V.V., Rozhkova, N.N., and Valley, J.W., *Can. Mineral.,* 1997, vol. 35, no. 6, pp. 1363–1378.
3. Ōsawa, E*., Pure Appl. Chem*., 2008, vol. 80, pp. 1365–1379.
4. Churaev, N.V. and Sobolev, V.D., *Colloid. J.*, 2005, vol. 67, no. 6, p. 764.
5. Estrela-Llopis, V.R., Borodinova, *T*.I., and Yurkova, I.N., *Kolloidno-khimicheskie osnovy nanonauki* (Colloid-Chemical Basics of Nanoscience), Shpak, A.P. and Ul'berg, Z.R., Eds., Kyiv: Akademperiodika, pp. 238–297.
6. *The Fullerenes: New Horizons for the Chemistry, Physics, and Astrophysics of Carbon*, Kroto, H.W. and Walton, D.R.M., Eds., Cambridge: Cambridge Univ., 1993.
7. Rozhkova, N.N., in *Perspectives of Fullerene Nanotechnology*, Ōsawa, E., Ed., Dordrecht: Kluwer Academic, 2002, pp. 237–251.
8. Geim, A.K., Science, 2009, no. 324, pp. 1530–1534.
9. Green, A.A. and Hersam, M.C., *Nano Lett.,* 2009, vol. 9, p. 4031; doi: 10.1021/nl902200b.
10. Qian, W., Hao, R., Hou, Y., Tian, Y., Shen, C., Gao, H., and Liang, X., *Nano Res*., 2009, no. 2, pp. 706–712.
11. Kovalevskii, V.V*., Doctoral (Geol.-Mineral.) Dissertation*, Syktyvkar, 2007.
12. Zaidenberg, A.Z., Kovalevski, V.V., and Rozhkova, N.N., *Proc. ECS Fullerene Symp*., 1995, pp. 24–27.
13. Alekseev, N.I., Arapov, O.V., Bodyagin, B.O., et al., *Russ. J. Appl. Chem*., 2006, vol. 79, no. 9, p. 1423.
14. Chiganova, G.A., *Colloid. J*., 2000, vol. 2, no. 2, p. 238.
15. Toporov, G.N., Semenov, M.V., Eliseeva, R.A., Khachatur'yan, *T*.K., and Tatarenko, V.A., *Kolloidn. Zh*., 1978, vol. 40, no. 3, pp. 575–577.

16. Kuchuk, V.I., Golikova, E.V., and Chernoberezhskii, Yu.M., *Kolloidn. Zh*., 1984, vol. 46, no. 6, pp. 1129–1135.
17. Morar, V.N., Ovcharenko, F.D., and Totskaya, L.A., *Kolloidn. Zh*., 1991, vol. 53, no. 5, pp. 874–879.
18. Park, S., An, J., Piner, R.D., Jung, I., Yang, D., Velamakanni, A., Nguyen, S.*T*., and Ruoff, R.S., *Chem. Mater*., 2008, vol. 20, no. 21, pp. 6592–6594.
19. Avdeev, M.V., Khokhryakov, A.A., Tropin, *T*.V., Andrievsky, G.V., Klochkov, V.K., Derevyanchenko, L.I., Rosta, L., Garamus, V.M., Priezzhev, V.B., Korobov, M.V., and Aksenov, V.L*., Langmiur*, 2004, vol. 20, no. 11, pp. 4363–4368.
20. Andrievsky, G.V., Kosevich, M.V., Vovk, O.M., Shelkovsky, V.S., and Vashenko, L.A., *J. Chem. Soc. Chem. Commun.,* 1995, vol. 12, pp. 1281–1282.
21. Alargova, R.G., Deguchi, Sh., and Tsujii, K*., J. Am. Chem. Soc*., 2001, vol. 123, no. 43, pp. 10460–10467.
22. Rozhkova, N.N., Emel'yanova, G.I., Gorlenko, L.E., Jankowska, A., Korobov, M.V., and Lunin, V.V., *Smart Nanocomposites*, 2010, vol. 1, no. 1, pp. 71–90.
23. Rozhkova, N.N., *Nanouglerod shungitov* (Shungite Nanocarbon), Petrozavodsk: Karel. Nauchn. Tsentr Ross. Akad. Nauk, 2011.
24. Emel'yanova, G.I., Gorlenko, L.E., Lunin, V.V., Tikhonov, N.A., Rozhkova, N.N., Rozhkova, V.S., and Lunin, V.V., *Russ. J. Phys. Chem., A*., 2004, vol. 78, no. 7, p. 1070.
25. Rozhkova, N.N., Rozhkova, V.S., Emel'yanova, G.I., Gorlenko, L.E., and Lunin, V.V., *Proc. 4th Int. Symp. "Fullerenes and Fullerene-Like Structures in Condensed Matter,"* Minsk, 2006, pp. 63–68.
26. Rozhkova, N.N., Rozhkova, V.S., Emelianova, G.I., Gorlenko, L.E., and Lunin, V.V*., Karbo*, 2007, vol. 52, no. 4, pp. 207–211.
27. Rozhkova, N.N., Gribanov, and A.V., Khodorkovskii, M.A., *Diamond Relat. Mater*., 2007, no. 16, pp. 2104–2108.
28. Lin, *T*., Zhang, W.-D., Huang, J., and He, Ch., *J. Phys. Chem. B.,* 2005, no. 109, pp. 13755–13760.
29. Ellison, M.D., Good, A.P., Kinnaman, C.S., and Padgett, N.E., *J. Phys. Chem. B*., 2005, no. 109, pp. 10640–10646.
30. Rozhkov, S.P., Kovalevskii, V.V., and Rozhkova, N.N., *Zh. Fiz. Khim*., 2007, vol. 81, no. 5, pp. 952–958.
31. Rozhkova, N.N. and Gribanov, A.V., *Materialy yubileinoi nauchnoi sessii, posvyashchennoi 45-letiyu Instituta geologii Karel'skogo Nauchnogo Tsentra Rossiiskoi Akademii Nauk i 35-letiyu Karel'skogo otdeleniya* (Proc. Jubilee Scientific Session Dedicated to the 45th Anniversary of the Institute of Geology, Karelian Scientific Center, Russian Academy of Sciences, and to the 35th Anniversary of the Karelian Branch), Petrozavodsk: Karel. Nauchn. Tsentr Ross. Akad. Nauk, 2007, pp. 6–89.
32. Rozhkov, S.P., Rozhkova, N.N., and Volkov, V.I*., Materialy II Rossiiskogo soveshchaniya "Organicheskaya mineralogiya"* (Proc. II Russ. Meeting "Organic Mineralogy"), Petrozavodsk, 2005, pp. 159–161.
33. Ziatdinov, A.M., *Ross. Khim. Zh*., 2004, vol. 48, no. 5, pp. 5–11.
34. Parfen'eva, L.S., Smirnov, I.A., Zaidenberg, A.Z., Rozhkova, N.N., and Stefanovich, G.B., *Fiz. Tverd. Tela*, 1994, vol. 36, no. 1, pp. 234–236.
35. Rozhkova, N.N., Abstracts of Papers, *Konferentsiya, posvyashchennaya 50-letiyu Instituta geologii Karel'skogo Nauchnogo Tsentra Rossiiskoi Akademii Nauk "Geologiya Karelii ot arkheya do nashikh dnei"* (Conf. Dedicated to the 50th Anniversary of the Institute of Geology, Karelian Scientific Center, Russian Academy of Sciences "Geology of Karelia from the Archean to the Present"), 2011, pp. 180–187.
36. Khairullin, A.R., Stepanova, *T*.P., Rozhkova, N.N., and Gladchenko, S.V., *Nauch.-Tekh. Vedom. Sankt-Peterb. Gos. Politekh. Univ*., 2012, no. 4 (158), pp. 111–114.
37. Rozhkova, N.N., Emel'yanova, G.I., Gorlenko, L.E., Gribanov, A.V., and Lunin, V.V., *Fiz. Khim. Stekla*, 2011, vol. 37, no. 6, pp. 853–859.
38. Emel'yanova, G.I., Gorlenko, L.E., Rozhkova, N.N., Rumyantseva, M.N., and Lunin, V.V., *Russ. J. Phys. Chem., A*., 2010, vol. 84, no. 8, p. 1376.
39. An, X., Simmons, *T*., Shah, R., Wolfe, Ch., Lewis, K.M., Washington, M., Nayak, S.K., Talapatra, S., and Kar, S., *Nano Lett*., 2010, vol. 10, no. 11, pp. 4295–4301.
40. Dementjev, A.P., Maslakov, K.I., and Naumkin, A.V., *Appl. Surf. Sci*., 2005, vol. 245, pp. 128–132.
41. Sheka, E.F. and Popova, N.A., *Graphane as Polyhydride of Graphene. Computational Synthesis Applied to Two-Side Membrane, arXiv:1102.0922 [cond-mat.mes-hall]*, 2011.
42. Popova, N.A. and Sheka, E.F., Abstracts of Papers, *Vos'maya mezhdunarodnaya konferentsiya "Uglerod: fundamental'nye problemy nauki, materialovedenie, tekhnologiya"* (Eighth Int. Conf. "Carbon: Fundamental Problems of Science, Materials Science, and Technology"), 2012, Troitsk, pp. 382–386.